Journal Pre-proof

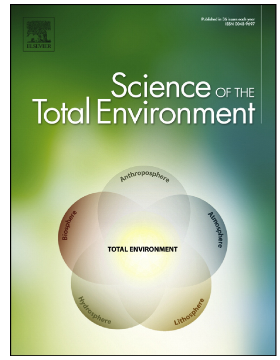

Temporal hydrochemical dynamics of the River Wensum, UK: Observations from long-term high-resolution monitoring (2011–2018)

Richard J. Cooper, Kevin M. Hiscock, Andrew A. Lovett, Stephen J. Dugdale, Gisela Sünnenberg, Emilie Vrain

PII: S0048-9697(20)31766-6

DOI: https://doi.org/10.1016/j.scitotenv.2020.138253

Reference: STOTEN 138253

To appear in: *Science of the Total Environment*

Received date: 13 December 2019

Revised date: 28 February 2020

Accepted date: 25 March 2020

Temporal Hydrochemical Dynamics of the River Wensum, UK: Observations from Long-term High-resolution Monitoring (2011–2018)

Richard J Cooper[1*], Kevin M Hiscock[1], Andrew A Lovett[1], Stephen J Dugdale[1], Gisela Sünnenberg[1], Emilie Vrain[1]

[1]*School of Environmental Sciences, University of East Anglia, Norwich Research Park, NR4 7TJ, UK*

*Correspondence: Richard.J.Cooper@uea.ac.uk

Graphical Abstract

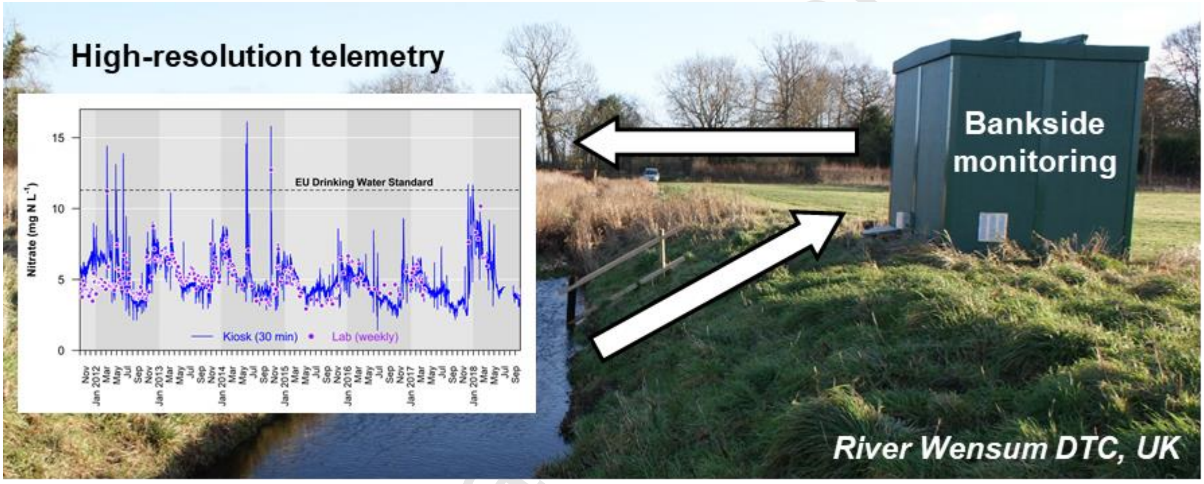

Abstract

In 2010, the UK government established the Demonstration Test Catchment (DTC) initiative to evaluate the extent to which on-farm mitigation measures can cost-effectively reduce the impacts of agricultural water pollution on river ecology while maintaining food production capacity. A central component of the DTC platform was the establishment of a comprehensive network of automated, web-based sensor technologies to generate high-temporal resolution (30 min) empirical datasets of surface water, groundwater and meteorological parameters over a long period (2011 – 2018). Utilising 8.9 million water quality measurements generated for the River Wensum, this paper demonstrates how long-term, high-resolution monitoring of hydrochemistry can improve our understanding of the complex temporal dynamics of riverine processes from 30-minute to annual timescales. This paper explores the impact of groundwater-surface water interactions on instream pollutant concentrations (principally nitrogen, phosphorus and turbidity) and reveals how varying hydrochemical associations under contrasting flow regimes can elicit important information on the dominant pollution pathways. Furthermore, this paper examines the relationships between agricultural pollutants and precipitation events of varying magnitude, whilst

demonstrating how high-resolution data can be utilised to develop conceptual models of hydrochemical processes for contrasting winter and summer seasons. Finally, this paper considers how high-resolution hydrochemical data can be used to increase land manager awareness of environmentally damaging farming operations and encourage the adoption of more water sensitive land management practices.

Keywords: High-frequency; Telemetry; Demonstration Test Catchment; Water Quality; Nitrate; Phosphorus.

1. Introduction

The importance of monitoring catchment water resources at high-frequency using automated, *in-situ*, telemetered technologies is increasingly being demonstrated by a growing number of studies published over the past decade (Blaen et al., 2016; Rode et al., 2016b). High-resolution monitoring (continuous-to-hourly) can provide important insights into both major and subtle aspects of catchment behaviour which can often be overlooked by conventional, lower resolution (daily-to-yearly) manual sampling (Halliday et al., 2014; Halliday et al., 2012). High-resolution monitoring can elucidate evidence of non-stationarity in biogeochemical processes (Aubert et al., 2016; Jarvie et al., 2018; Neal et al., 2013; Yang et al., 2019; Zimmer et al., 2019), uncover hysteresis patterns in sediment and nutrient concentrations (Bieroza and Heathwaite, 2015; Bowes et al., 2015; Lloyd et al., 2016a), identify periods of pollutant storage and mobilisation pathways (Burns et al., 2019; Krause et al., 2015; Mellander et al., 2012), and reveal the intricate dynamics of storm-dependent pollutant transfers (Bhurtun et al., 2019; Blaen et al., 2017; Outram et al., 2014; Strohmeier et al., 2013). High-resolution hydrochemical monitoring is also particularly valuable for providing evidence on the effectiveness of water pollution mitigation measures to support environmental policy-making decisions (Cooper et al., 2019; Cooper et al., 2017; Drake et al., 2018; Lloyd et al., 2014) and in classifying waterbody status for legislative purposes (e.g. EU Water Framework Directive standards; (Halliday et al., 2015; Skeffington et al., 2015). High-resolution monitoring can also have considerable social and economic benefits through the monitoring of river discharge upstream of urban areas, which can serve as a valuable early warning system for authorities seeking to alleviate the deleterious impacts of flooding on local communities (Castillo-Effen et al., 2004; Fekete et al., 2012; Marin-Perez et al., 2012).

Ultimately, however, the temporal frequency at which river systems are monitored depends upon the expected degree of variability in the parameters being assessed, the purpose of the monitoring and the resources available to make quantitative measurements. High-resolution monitoring is usually expensive to conduct due to either the high capital costs of installing, maintaining and running suitable instrumentation, or due to high labour costs from time-consuming sample collection and processing (Blaen et al., 2016; Rode et al., 2016b). These costs typically render high-resolution analysis unsuitable for many water resource monitoring programmes where the need for it is not essential and financial resources are constrained. Low-resolution monitoring is cheaper, quicker to conduct, easier to deploy over a wider geographical area and can elucidate important information on the underlying background state and thereby provide a useful benchmark with which to compare between sites monitored at comparable resolutions (Bieroza et al., 2014; Bowes et al., 2018; Dupas et al., 2018). However, low-resolution monitoring fails to capture the full range of pollutant concentrations and waterbody conditions, and can lead to a systematic bias in water quality interpretation (Cassidy and Jordan, 2011; Lloyd et al., 2016b), especially if water samples degrade in the time between on-site sample collection and analysis in the laboratory (Bieroza and Heathwaite, 2016).

Established in 2010, the Demonstration Test Catchment (DTC) platform was a UK government initiative funded by the Department for Environment, Food and Rural Affairs (Defra) working in four English catchments to evaluate the extent to which on-farm mitigation measures can cost-effectively reduce the impacts of agricultural water pollution on river ecology while maintaining food production capacity (McGonigle et al., 2014). Each DTC focussed on a different type of farming system, namely, intensive arable (River Wensum DTC, Norfolk), upland livestock (River Eden DTC, Cumbria) and mixed farming (River Avon DTC, Hampshire; River Tamar DTC, Devon/Cornwall). A central component of the DTC platform was the establishment of a comprehensive network of automated, web-based sensor technologies to generate high-temporal resolution (30 min) empirical datasets of surface water, soil water, groundwater and meteorological parameters over a long time period (2011 – 2018) in order to accurately assess the efficacy of on-farm mitigation measures (Lovett et al., 2015; Cooper et al., 2017; Cooper et al., 2018; Cooper et al., 2019; Cooper et al., 2020).

Focusing on the River Wensum DTC, the aim of this paper is to demonstrate how long-term, high-resolution, hydrochemical monitoring can improve our understanding of the complex temporal dynamics of riverine processes. Specifically, this paper aims to:

(i) Investigate the temporal hydrochemical dynamics of the River Wensum at hourly-to-seasonal timescales over a seven year period (2011 – 2018);

(ii) Assess how hydrochemical associations vary under contrasting high (Q_{10}) and low (Q_{90}) discharge regimes;

(iii) Explore groundwater-surface water interactions and the response of surface water hydrochemistry to precipitation events;

(iv) Demonstrate how high-resolution data can be used to develop conceptual models of hydrochemical processes;

(v) Consider how high-resolution hydrochemical data can be utilised to encourage the adoption of water sensitive land management practices.

2. Methods

2.1 River Wensum

The River Wensum, UK, is a 78 km length lowland, calcareous river that drains an area of 660 km^2, with a mean discharge of 4.1 m^3 s^{-1} at its outlet and annual baseflow indices (BFI) ranging from 0.5 to 0.9 (CEH, 2017). The River Wensum is designated a Site of Special Scientific Interest (SSSI) and European Special Area of Conservation (SAC) due to the diversity of its internationally important flora and invertebrate fauna and in recognition of it being one of the best examples of a lowland calcareous river system in the UK (Grieve et al., 2002; Sear et al., 2006). The River Wensum catchment comprises 20 sub-catchments, one of which, the 19.7 km^2 Blackwater Drain, represents the area intensively studied as part of the River Wensum DTC and provides the focus of this paper (**Figure 1**). At its outlet, the Blackwater Drain has a mean discharge of 0.098 m^3 s^{-1} and a mean annual BFI of 0.64 to 0.70. For monitoring purposes, the Blackwater Drain is divided into six mini-catchments named *A* to *F*, across which there are pronounced contrasts in the superficial geology and soil type (Cooper et al., 2018; Lewis, 2014).

The western section (mini-catchments A + B) is underlain by a complex sequence of Mid-Pleistocene chalky, flint-rich, argillaceous glacial tills of the Sheringham Cliffs (0.2 – 7 m depth) and Lowestoft (8 – 16 m depth) Formations, with interdigitated bands of glaciofluvial and glaciolacustrine sands and gravels. In turn, these are superimposed onto the quartzite-rich marine sands and gravels of the Lower Pleistocene Wroxham Crag Formation (16 – 22 m depth), which overlies Cretaceous Chalk (>22 m depth). The soils are predominantly clay loams of the argillic brown earths and stagnogley groups which, together with the argillaceous tills, result in moderately impeded drainage conditions in this western section. Most of the arable land in this western section is therefore extensively under-drained by a dense network (43 outflows per km of river) agricultural field drains installed in a herringbone layout at depths of 100 – 150 cm during numerous phases of land drainage over past decades. Drain flow rates vary depending on antecedent conditions, but most drains flow between October and March at discharges of up to 10 L s^{-1}, with limited flow during April to September.

In contrast, the eastern section (mini-catchments C + D) is more freely draining with sheets of glacial outwash sands and gravels of the Mid-Pleistocene Briton's Lane Formation (0.2–7 m depth) overlying the clay-rich Bacton Green Till Member (6–10 m depth), interdigitated with higher permeability glaciolacustrine sands (8–10 m depth). Underlying this are the glaciofluvial, glaciolacustrine and glaciogenic sands, gravels and tills of the Happisburgh Formation (12–17 m depth). Lastly, as in the western section, the Wroxham Crag Formation (17–22 m depth) overlies Cretaceous Chalk (>22 m depth). The soils in the eastern section are predominately freely draining sandy loams of the brown sands and brown earth groups.

Situated 30-50 m above sea level and with gentle slopes that rarely exceed 0.5^{o} of inclination, land use in the Blackwater Drain is dominated by intensive arable cultivation, ranging from 60% on the lower fertility sandy loam soils of mini-catchment C, to 92% on the fertile clay loam soils of mini-catchment A. Winter wheat, winter and spring barley, sugar beet, oilseed rape and spring beans are the dominant crop types, with these being grown in a seven-year rotation across much of the western half of the sub-catchment. The remainder of the land use is comprised of improved grassland (12%), rough grassland (2%), mixed woodland (11%), freshwater (<1%) and a collection of small rural settlements with a population of ~100 people (1%).

2.2 Riverine Monitoring

At the outlet of the six Blackwater Drain mini-catchments (sites A – F) bankside monitoring stations recorded semi-continuous measurements of river water quality parameters at 30-min resolution (**Figure 2**). All monitoring stations measured temperature, conductivity, pH, turbidity, dissolved oxygen and ammonium via multi-parameter sondes (YSI 6600) mounted in flow-through cells. In addition, two larger main monitoring stations at sites E and F measured nitrate-N (Hach Lange Nitratax SC optical probe), total phosphorus (TP) and total reactive phosphorus (TRP) (Hach Lange Sigmatax SC combined with Phosphax Sigma). River stage was measured using pressure transducers housed in stilling wells (Impress IMSL Submersible Level Transmitter) and was converted into river discharge via stage-discharge rating curves constructed from manual flow gauging with an open-channel EM flow meter. Collectively, these monitoring stations made 8.9 million high-frequency measurements between October 2011 and September 2018. All data were uploaded to a web-based server in near real-time via a wireless telemetry system (Meteor Communications Ltd.). Further details of the hydrochemical monitoring are provided in Outram et al. (2016).

2.3 Groundwater monitoring

Groundwater data were generated from two sets of boreholes which capture the influence of the different geologies between the eastern and western parts of the catchment. The western set of boreholes (Merrisons Lane MLBH1–4) were drilled to depths of 50 m (Chalk), 15 m (Lowestoft Formation), 12 m (Sheringham Cliffs Formation – sands and gravels) and 4 m (Sheringham Cliffs Formation – Bacton Green Till Member). The eastern set (Park Farm PFBH1–4) were drilled to depths of 48 m (Chalk), 17 m (Happisburgh Formation – sands and gravels), 10 m (Sheringham Cliffs Formation – sands and gravels) and 6 m (Britons Lane Formation). Each borehole was equipped with a pressure transducer (Mini-Diver, Schlumberger) which recorded temperature and pressure at 15-min resolution and was manually downloaded every 2–3 months and barometrically compensated by linear interpolation using the barometer located at each borehole set (BARO, Schlumberger).

2.4 Meteorological Monitoring

Meteorological data at 15-min resolution were generated from two weather stations installed in mini-catchments A and D (**Figure 1**). These recorded precipitation via tipping-bucking rain gauges, alongside measurements of temperature, wind speed, humidity and net solar radiation. In addition, five further tipping bucket rain gauges distributed across the sub-catchment also recorded precipitation at 15-min intervals and these data were compiled into a single master record based on the median of the seven records. All weather station data were also uploaded to web-based servers via wireless telemetry (Meteor Communications Ltd.; Isodaq Technology). During the study period (2011 – 2018), the mean annual temperature was 10.1^{o}C and the mean annual precipitation total was 680 mm. Annual hydrological year (Oct – Sep) precipitation totals were 694 mm (2011/12), 638 mm (2012/13), 724 mm (2013/14), 715 mm (2014/15), 742 mm (2015/16), 632 mm (2016/17) and 616 mm (2017/18). Further details on the hydrometerological monitoring are presented in Cooper et al. (2018).

2.5 EU Water Framework Directive Status

The EU Water Framework Directive (2000/60/EC) had the original aim to ensure that all waterbodies within member states must achieve '*good'* qualitative and quantitative status by 2015. However, by 2015 only 53% of waterbodies were meeting this target which represented just a 10% improvement since 2000 (Halliday et al., 2015; Voulvoulis et al., 2017). Consequently, many member states have since applied for extensions to the end of the second (2015 – 2021) and third (2021 – 2027) management cycles in order to achieve this goal. Here, the physico-chemical status of the Blackwater Drain was assessed against the WFD metrics. For classification purposes, the Blackwater Drain is designated as a small (10-100 km^2 catchment), lowland (mean altitude <200 m), calcareous river system with water quality standards for nitrate, total reactive phosphorus, dissolved oxygen, temperature and pH given in **Table 1**.

3. Results

3.1 Seasonal Cycles

Time series of the high-resolution hydrochemical data generated for the Blackwater Drain at site F between October 2011 and September 2018 are shown in **Figure 3** and summarised in **Table 2**. Strong seasonality was recorded in river discharge with mean winter flows (0.133 $m^3 s^{-1}$) significantly ($p < 0.05$) greater than summer flows (0.029 $m^3 s^{-1}$) due to increased summer evaporative losses and lower groundwater levels reducing baseflow input. Water temperatures also displayed a strong seasonal cycle in response to solar radiation, with a mean summer water temperature (14.0^{o}C) more than double the winter average (6.1^{o}C). This seasonal variability in temperature resulted in seasonal variability in dissolved oxygen concentrations, which ranged from a mean high of 96% during the winter to 86% in the summer and 83% in the autumn as higher temperatures and lower flow reduced oxygen solubility. Conductivity and pH were also significantly ($p < 0.05$) higher in winter than in summer, which can be explained by more carbonate dissolved in the water during winter due to greater flushing of carbonate-rich soil water and erosion of the carbonate-rich riverbed and channel banks.

With respect to nutrients, riverine nitrate concentrations were found to display a strong seasonal cycle, with significantly ($p < 0.05$) higher mean concentrations observed during the winter (6.4 mg N L^{-1}) compared to the summer (4.3 mg N L^{-1}). This principally occurs due to winter rainfall readily leaching soil nitrate into the shallow groundwater beneath fallow arable fields from where it discharges into the river, either through the subsurface agricultural field drains or via upwelling through the riverbed (Burns et al., 2019; Di and Cameron, 2002; Outram et al., 2014). During the spring and summer, the reverse situation occurs as rapidly growing crops absorb excess nitrate and convert it into organic nitrogen, thus leaving little residual nitrate within the soil to be leached into the groundwater. However, this was not always the case, as large summer storm events initiated a flushing of nitrate through the river system, displacing nitrate stored within the catchment (e.g. in riverbed sediments) during the preceding months of lower flow conditions and resulting in very high peaks in summer nitrate concentration (note the nitrate peak in June 2014 in **Figure 3**).

In contrast, total phosphorus and total reactive phosphorus concentrations displayed more subtle seasonality, with mean concentrations marginally higher during the summer (TP = 0.109 mg L^{-1}; TRP = 0.079 mg L^{-1}) and lower during the winter (TP = 0.082 mg L^{-1}; TRP = 0.068 mg L^{-1}). This can be explained by the accumulation of organic phosphorus within the river channel during the summer months due to the rapid growth of primary producers and subsequent phosphorus cycling driven by bacterial decomposition (Withers and Jarvie, 2008). Additionally, whilst there are no sewage treatment works within the catchment, most houses are served mainly by septic tanks which can leak if poorly maintained and contribute to high phosphorus concentrations during summer low-flows (Jarvie et al., 2006). The dominant temporal trend in both phosphorus concentrations and turbidity, however, was highly flashy with concentrations strongly linked to individual rainfall events which trigger soil erosion and/or the movement of sediment-bound phosphorus stored upon the riverbed (Ballantine et al., 2009; Dupas et al., 2015a; Dupas et al., 2015b).

Mean turbidity values were highest in spring (9.3 NTU) and lowest in autumn (5.5 NTU), likely reflecting in part the positive correlation between turbidity and chlorophyll concentrations (r = 0.46) which were also lowest in autumn (4.3 µg L^{-1}) and highest in spring (5.3 µg L^{-1}). Perhaps surprising, however, mean turbidity values were marginally lower during winter (7.4 NTU), when soil erosion rates are typically higher, than during summer (7.5 NTU). This can partly be explained by the increasing concentration of suspended particulate matter (SPM) under low summer flow conditions, thus increasing turbidity, whilst SPM is partly diluted during higher winter flows, but only during periods of no precipitation (Stutter et al., 2008).

3.2 Diel Cycles

A wide variety of hydrochemical parameters in river systems are known to exhibit diel cycles in response to both biotic and abiotic processes (Nimick et al., 2011; Palmer-Felgate et al., 2008). Here, diel cycles in the hydrochemistry of the Blackwater Drain, differentiated by season, are shown in **Figure 4** for the ten high-resolution parameters recorded by the bankside monitoring station. Pronounced diel cycles were recorded for five parameters (temperature, dissolved oxygen, pH, turbidity, chlorophyll) with more subtle diel cycles exhibited for phosphorus, but in all cases the extent of this behaviour varied depending upon season. Three parameters (discharge, conductivity and nitrate concentration) exhibited negligible diel cycles.

Strong diel cycles in dissolved oxygen and pH during the spring and summer are driven by photosynthetic oxygen production and CO_2 absorption during the day, resulting in an oxygen and pH maxima at 12:00–14:00. Conversely, during the night a shift to a respiration dominated system produces a dissolved oxygen and pH minima at 22:00–00:00 as an increase in dissolved CO_2 increases water acidity (Nimick et al., 2011). Evidence of biological activity can also be seen in the chlorophyll concentrations which peaked strongly around midday (11:00–13:00) during spring and summer as primary production responds to increased solar radiation and higher water temperatures. As these primary producers photosynthesise during the summer months they assimilate phosphorus which produces a subtle minima in both TP and TRP during the day (10:00–12:00) and corresponding maxima at night (22:00– 23:00) as plant uptake reduces dissolved nutrient concentrations (Withers and Jarvie, 2008).

Further evidence of biological activity can be seen in the turbidity data which displays a maxima at night (21:00–22:00) and a minima during the day (11:00–12:00), with this being especially pronounced during the summer and autumn (**Figure 6**). Previous studies have associated this with nocturnal bioturbation by aquatic fauna, particularly the invasive North American signal crayfish (*Pacifastacus leniusculus*), which forages for food in the sediment on the riverbed whilst also excavating burrows into the riverbank at night (Cooper et al., 2016a; Harvey et al., 2014; Rice et al., 2016; Turley et al., 2017). The absence of a night-time turbidity maxima during the colder winter months can be explained by the reduced activity of nocturnal organisms. However, the reason for a prominent peak in winter turbidity at 08:00–09:00 is unclear, although it appears to be caused by localised sediment disturbance as such a turbidity peak was not recorded upstream at site E.

Interestingly, in contrast to previous studies (Aubert and Breuer, 2016; Rode et al., 2016a), no diel cycle was evident in nitrate concentrations suggesting that riverine nitrate at this location was largely controlled by non-biotic processes occurring more widely across the catchment. There was, however, some evidence of nocturnal denitrification recorded upstream at monitoring site E during the warmer summer months when lower dissolved oxygen concentrations resulted in conditions conducive to hypoxic denitrification (**Figure SM1**). At this time, discharge also displayed a subtle diel cycle as a result of evapotranspirative losses in the riparian zone resulting in reduced river flows around midday until 23:00.

3.3 Hydrochemical associations under contrasting flow regimes

Examining the relationships between hydrochemical parameters measured at 30 minute resolution under high (Q_{10}) and low (Q_{90}) discharge regimes can reveal important insights into the dominant catchment processes occurring under contrasting hydrological conditions. For nitrate, **Figure 5** and **Figure 6** reveal that concentrations were weakly correlated with discharge under both high- (r = 0.24) and low-flow (r = 0.05) regimes. High-flow storm events were dominated by anticlockwise hysteresis loops caused by peak nitrate occurring on the recession limb of the hydrograph, indicating nitrate transport either via slower pollution pathways (e.g. subsurface leaching) or nitrate pollution derived from distal sources. No such nitrate-discharge hysteresis was present during Q_{90} conditions due to the lack of precipitation induced pollutant mobilisation. Nitrate concentrations were, however, more strongly negatively correlated (r = -0.44) with water temperatures during low-flow conditions, with higher temperatures during summer low-flows conducive to increased denitrification due to reduced oxygen solubility and more hypoxic conditions.

TP and TRP were strongly positively correlated (r = > 0.78) with turbidity under both high- and low-flows, indicating the sorption of phosphorus onto the surfaces of iron and aluminium oxyhydroxides present in fine-grained suspended particulate matter (Cooper et al., 2015b). TP (r = 0.56) and turbidity (r = 0.70) also exhibited strong positive correlation with discharge under Q_{10} conditions, with clockwise hysteresis loops during these high-flows indicating either the activation of rapid transport pathways (e.g. surface runoff) during rainfall events or sediment-bound phosphorus being delivered from sources in close proximity to the river channel. Phosphorus and turbidity were also strongly negatively correlated (r = -0.54 – 0.76) with conductivity during both flow regimes, a relationship which provides an indication of the likely source of sediment-bound phosphorus in the Blackwater Drain. Conductivity increases during low-flow conditions when most SPM is derived from the erosion of carbonate-rich river channel banks which are depleted in phosphorus but which increase the conductivity and pH of the water (Cooper et al., 2015a). Conversely, during precipitation events, SPM is largely derived from erosion of surface sources depleted in carbonate, hence lower conductivity, and enriched in phosphate. Lastly, TP, TRP, turbidity and chlorophyll were all moderately positively correlated with water temperature during Q_{90} conditions (r = >0.44), which likely reflects higher primary productivity during warm summer low-flows and increased production of organic phosphorus.

3.4 Groundwater and Surface Water Interaction

The hydrology of the Blackwater Drain is strongly groundwater dominated (BFI = 0.64 – 0.70) and the river consequently exhibits prominent groundwater – surface water interactions. **Figure 7** highlights the relationships between mean daily shallow (4 m depth) groundwater level within the Merisons Lane borehole and mean daily river discharge, nitrate concentration, total phosphorus concentration and turbidity within the Blackwater Drain at site F. River discharge was observed to be strongly exponentially correlated to groundwater level (R^2 = 0.645), with discharge being largely unresponsive to changing groundwater levels between 39.5 and 42.0 m above sea level (asl). However, once the groundwater level rose above 42 m asl and to within 1 m of the ground surface (43 m asl), river discharge increased exponentially. This increase at 42 m asl is hydrologically important as it represents the height at which the surface of the shallow groundwater table is intercepted by the subsurface agricultural field drainage network which provides an artificial, preferential quickflow pathway for groundwater transport into the Blackwater Drain.

Mean daily river nitrate concentration was also observed to be strongly exponentially correlated (R^2 = 0.489) with groundwater level, although less so than discharge. Nitrate concentrations increased markedly once groundwater levels rose above 42 m asl, highlighting the mechanism by which subsurface field drainage directs nitrate leaching through the soil profile into these preferential pathways for rapid transport into the surface water environment. Conversely, both total phosphorus (R^2 = 0.037) and turbidity (R^2 = 0.006) were unaffected by changes in shallow groundwater levels, reflecting that sediment-bound phosphorus is predominantly transported via surface runoff pathways and is therefore largely unaffected by rising groundwater levels unless it saturates soil surface – a process which is largely inhibited in this catchment due to field drainage keeping groundwater levels below 0.5 m depth.

3.5 Precipitation and Surface Water Interaction

Although the Blackwater Drain is groundwater dominated, surface runoff nevertheless accounts for 30–36% of total discharge and storm event pollutant transport still heavily impacts upon river water quality (**Figure SM2**). **Figure 8** shows the relationships between daily precipitation total and the percentage change in daily discharge, nitrate concentration, TP concentration and turbidity in the Blackwater Drain differentiated by season. This reveals changes in daily discharge to be strongly positively correlated with daily precipitation, especially during the autumn (R^2 = 0.734), winter (R^2 = 0.653) and spring (R^2 = 0.691), whilst summer correlation is notably weaker (R^2 = 0.435). These seasonal differences likely reflect contrasting soil moisture conditions, with higher soil moisture levels during the late autumn, winter and early spring months resulting in a more precipitation responsive system whereby rainfall onto wet soils readily triggers surface runoff and infiltration into the subsurface field drain network. Conversely, during the summer, higher rates of evapotranspiration result in reduced soil moisture levels and a less responsive system, whereby precipitation does not trigger surface runoff and infiltration as readily (Cooper et al., 2018).

A very similar pattern was observed for nitrate, TP and turbidity, all of which were more strongly correlated with daily precipitation totals during the autumn to spring months (**Figure 8**). The reduced sensitivity of nitrate to summer rainfall highlights a less active summer leaching pathway, whilst the reduced sensitivity of TP and turbidity indicate less active summer surface runoffs pathways. Further evidence in support of these dominant pollution transport mechanisms can be inferred from the mean changes in daily pollutant concentrations. Whilst daily nitrate concentrations increased by an average of just 10.8% (range = 0% to 363%) above pre-event conditions in response to daily rainfall totals, total phosphorus increased by 70.1% (range = 0% to 1260%) and turbidity by 183.8% (range = 0% to 3629%), clearly emphasising the more dominant role of precipitation induced surface runoff in the mobilisation of soils and sediment-bound phosphorus compared to the dominance of subsurface leaching and groundwater interactions for nitrate (see section 3.4).

4. Discussion

4.1 Developing Conceptual Models

Utilising the information obtained from the high-resolution monitoring, it is possible to develop conceptual models of catchment hydrochemical processes within the Blackwater Drain during contrasting summer and winter seasons (**Figure 9**). During winter, the Blackwater Drain is characterised by high nitrate concentrations as a combination of precipitation-induced leaching and elevated groundwater levels activate quickflow through subsurface agricultural field drains beneath exposed arable fields, resulting in the discharge of dissolved nitrate directly into the river. Saturated soils due to low rates of evapotranspiration increase surface runoff potential and the delivery of sediment-bound phosphorus into the river channel. However, high river discharge initiates flushing of sediment and sediment-bound phosphorus from the riverbed, moving material down the Blackwater Drain and into the main River Wensum. This flushing also erodes the carbonate-rich riverbed and channel banks leading to elevated pH and electrical conductivity. Low air temperatures and low solar radiation reduce water temperature and increase oxygen solubility leading to high dissolved oxygen concentrations despite limited photosynthetic oxygen production from primary productivity.

Conversely, during the summer, the Blackwater Drain is characterised by low nitrate concentrations as a fall in groundwater levels deactivates field drain quickflows and extensive arable crop growth absorbs excess nitrogen within the soil (**Figure 9**). Increased evapotranspiration reduces soil saturation, thereby lowering surface runoff potential and thus reducing the transport of sediment-bound phosphorus into the river. Low river discharge and limited flushing leads to increased sediment storage on the riverbed which can become mobilised during large summer storm events. Increased air temperatures and solar radiation increase water temperature and reduce oxygen solubility, leading to lower dissolved oxygen concentrations. However, increased primary productivity causes strong diel cycles in the hydrochemistry as high rates of photosynthesis result in pronounced peaks in pH, dissolved oxygen and chlorophyll concentration around midday. Increased water temperatures also triggers increased bioturbation, which causes nocturnal peaks in turbidity as aquatic fauna disturb riverbed and channel bank sediments.

4.2 Physico-chemical Status

Applying the EU Water Framework Directive standards to the full high-resolution dataset reveals the Blackwater Drain has a moderate-to-poor physico-chemical status with respect to nutrients (**Figure 10**). Although the EU Drinking Water Directive (98/83/EC) standard for nitrate was exceeded just 0.4% of the time, for 29.1% of the time nitrate concentrations were *'poor'* and for 57.4% of the time concentrations were '*moderate'*. Crucially, for only 13.1% of the time, water quality in the Blackwater Drain achieved the target '*good'* chemical status with respect to nitrate. TRP concentrations were slightly better, being '*poor'* for just 0.6% of the time, *'moderate'* for 62.6% of the time and achieving the target '*good'* status for 36.7% of the time. In contrast, the generally cool, alkaline and well-oxygenated waters of the Blackwater Drain meant that water quality status was '*high'* for temperature, pH and dissolved oxygen for almost 100% of the time between October 2011 and September 2018. From a legislative perspective, it can therefore be concluded that the Blackwater Drain failed to meet *'good'* physico-chemical status during this seven-year period due to excessive nutrient enrichment from the surrounding agricultural land. The adoption of on-farm mitigation measures to reduce land-to-river nutrient transfers is therefore essential if the Blackwater Drain is to achieve '*good'* status by 2021 or 2027.

4.3 Influencing Land Management Behaviour

To understand the value to land managers of high-resolution monitoring, qualitative data were collected through interviews with two farm managers directly involved in the River Wensum DTC. The farm managers elicited how they would not have considered investing in hydrochemical data collection before their involvement in the DTC project, but now in light of their experience, they have entirely developed their farming system based on these high-resolution data, claiming the data "*have been utterly invaluable for our decision making*". The most influential evidence generated was said to be the near real-time data which clearly showed nutrient losses from their fields: "*The data of what is coming out of the field drainage was a shock. During one day, we discovered we had lost six tonnes of nitrogen. It has certainly engaged all the staff and motivated us to be more efficient and mindful of our actions.*" Having local high-resolution data available and discovering how detrimental the timing of field activities can be has taught the farmers to be patient, giving them the confidence that it is better to do nothing than, for example, cultivate the soil in wet weather and potentially damage the soil structure. Additionally, discovering the benefits and successes of specific mitigation measures through the data collected has resulted in wider adoption across the farm outside of the DTC experimental area. Overall, the ability to be able to provide land managers with high-resolution hydrochemical datasets capable of clearly demonstrating how land management practices impact upon water resources can help to significantly improve awareness and thus promote increased adoption of water sensitive farming techniques (Inman et al., 2018).

5. Conclusions

This study has demonstrated how long-term, high-resolution monitoring of fluvial hydrochemistry can improve our understanding of the complex temporal dynamics of riverine processes from 30-minute to annual timescales. In particular, the investigation of diel cycles, analysis of groundwater-surface water interactions, interpretation of flow-dependant hydrochemical associations, and the formulation of relationships between instream pollutants and precipitation magnitude were all only possible through the use of automated, high-resolution, *in-situ* sensor technology. The development of new *in-situ* technologies capable of measuring a wider suite of hydrochemical parameters than those presented here, such as pesticides, micronutrients and even DNA (Rode et al., 2016b), will greatly enhance our understanding of riverine hydrochemical processes and further increase justification for the widespread use of these sensors. The benefits compared with traditional low-resolution (e.g. weekly or monthly; **Figure SM3**) manual sampling are clear, both scientifically, in terms of enhancing our understanding of hydrological systems, and socially, with respect to increasing stakeholder engagement and encouraging beneficial land management change. However the logistical and financial constraints to the adoption of these technologies for typical regulatory catchment-scale monitoring programmes still largely remain and efforts must continue to ensure that future technologies are both technically and financially advantageous.

Acknowledgements

This research was funded by the UK Department for Environment, Food and Rural Affairs (Defra) under the Demonstration Test Catchments initiative (WQ0212/WQ0225/LM0304). The authors would like to thank the Salle Park Estate and the Heydon Estate for their cooperation in hosting the monitoring equipment and Lister Noble for providing farm liaison support. We thank Liz Rix, Alina Mihailova, Kim Goodey, Tony Hinchliffe, Graham Chilvers and Andy Hind for the laboratory analysis and Faye Outram, Jenny Stevenson, Simon Ellis, Nick Garrard and Steve Warnes for their fieldwork support.

References

Aubert AH, Breuer L. New Seasonal Shift in In-Stream Diurnal Nitrate Cycles Identified by Mining High-Frequency Data. PLoS One 2016; 11: e0153138, doi: 10.1371/journal.pone.0153138.

Aubert AH, Thrun MC, Breuer L, Ultsch A. Knowledge discovery from high-frequency stream nitrate concentrations: hydrology and biology contributions. Sci Rep 2016; 6: 31536, doi: 10.1038/srep31536.

Ballantine DJ, Walling DE, Collins AL, Leeks GJL. The content and storage of phosphorus in fine-grained channel bed sediment in contrasting lowland agricultural catchments in the UK. Geoderma 2009; 151: 141-149, doi: 10.1016/j.geoderma.2009.03.021.

Bhurtun P, Lesven L, Ruckebusch C, Halkett C, Cornard JP, Billon G. Understanding the impact of the changes in weather conditions on surface water quality. Sci Total Environ 2019; 652: 289-299, doi: 10.1016/j.scitotenv.2018.10.246.

Bieroza MZ, Heathwaite AL. Seasonal variation in phosphorus concentration–discharge hysteresis inferred from high-frequency in situ monitoring. Journal of Hydrology 2015; 524: 333-347, doi: 10.1016/j.jhydrol.2015.02.036.

Bieroza MZ, Heathwaite AL. Unravelling organic matter and nutrient biogeochemistry in groundwater-fed rivers under baseflow conditions: Uncertainty in in situ high-frequency analysis. Sci Total Environ 2016; 572: 1520-1533, doi: 10.1016/j.scitotenv.2016.02.046.

Bieroza MZ, Heathwaite AL, Mullinger NJ, Keenan PO. Understanding nutrient biogeochemistry in agricultural catchments: the challenge of appropriate monitoring frequencies. Environ Sci Process Impacts 2014; 16: 1676-91, doi: 10.1039/c4em00100a.

Blaen PJ, Khamis K, Lloyd C, Comer-Warner S, Ciocca F, Thomas RM, et al. High-frequency monitoring of catchment nutrient exports reveals highly variable storm event responses and dynamic source zone activation. Journal of Geophysical Research: Biogeosciences 2017; 122: 2265-2281, doi: 10.1002/2017jg003904.

Blaen PJ, Khamis K, Lloyd CEM, Bradley C, Hannah D, Krause S. Real-time monitoring of nutrients and dissolved organic matter in rivers: Capturing event dynamics, technological opportunities and future directions. Sci Total Environ 2016; 569-570: 647-660, doi: 10.1016/j.scitotenv.2016.06.116.

Bowes MJ, Armstrong LK, Harman SA, Wickham HD, Nicholls DJE, Scarlett PM, et al. Weekly water quality monitoring data for the River Thames (UK) and its major tributaries (2009–2013): the Thames Initiative research platform. Earth System Science Data 2018; 10: 1637-1653, doi: 10.5194/essd-10-1637-2018.

Bowes MJ, Jarvie HP, Halliday SJ, Skeffington RA, Wade AJ, Loewenthal M, et al. Characterising phosphorus and nitrate inputs to a rural river using high-frequency concentration-flow relationships. Sci Total Environ 2015; 511: 608-20, doi: 10.1016/j.scitotenv.2014.12.086.

Bowes MJ, Smith JT, Neal C. The value of high-resolution nutrient monitoring: A case study of the River Frome, Dorset, UK. Journal of Hydrology 2009; 378: 82-96, doi: 10.1016/j.jhydrol.2009.09.015.

Burns DA, Pellerin BA, Miller MP, Capel PD, Tesoriero AJ, Duncan JM. Monitoring the riverine pulse: Applying high-frequency nitrate data to advance integrative understanding of biogeochemical and hydrological processes. Wiley Interdisciplinary Reviews: Water 2019: e1348, doi: 10.1002/wat2.1348.

Cassidy R, Jordan P. Limitations of instantaneous water quality sampling in surface-water catchments: Comparison with near-continuous phosphorus time-series data. Journal of Hydrology 2011; 405: 182-193, doi: 10.1016/j.jhydrol.2011.05.020.

Castillo-Effen M, Quintela DH, Jordan R, Westhoff W, Moreno W. Wireless sensor networks to flash-flood alterting. Proceedings of the Fifth IEEE International Caracas Conference on Devices, Circuits and Systems 2004: 5

Cooper RJ, Hama-Aziz ZQ, Hiscock KM, Lovett AA, Vrain E, Dugdale SJ, Sünnenberg G, Dockerty T, Hovesen P, Noble L. Conservation tillage and soil health: lessons from a 5-year UK farm trial (2013-2018). *Under review in Soil & Tillage Research* 2020.

Cooper RJ, Battams ZM, Pearl SH, Hiscock KM. Mitigating river sediment enrichment through the construction of roadside wetlands. J Environ Manage 2019; 231: 146-154, doi: 10.1016/j.jenvman.2018.10.035.

Cooper RJ, Hama-Aziz Z, Hiscock KM, Lovett AA, Dugdale SJ, Sünnenberg G, et al. Assessing the farm-scale impacts of cover crops and non-inversion tillage regimes on nutrient losses from an arable catchment. Agriculture, Ecosystems & Environment 2017; 237: 181-193, doi: 10.1016/j.agee.2016.12.034.

Cooper RJ, Hiscock KM, Lovett AA, Dugdale SJ, Sünnenberg G, Garrard NL, et al. Application of high-resolution telemetered sensor technology to develop conceptual models of catchment hydrogeological processes. Journal of Hydrology X 2018; 1: 100007, doi: 10.1016/j.hydroa.2018.100007.

Cooper RJ, Krueger T, Hiscock KM, Rawlins BG. High-temporal resolution fluvial sediment source fingerprinting with uncertainty: a Bayesian approach. Earth Surf. Process. Landforms 2015a; 40: 78-92, doi: 10.1002/esp.3621.

Cooper RJ, Outram FN, Hiscock KM. Diel turbidity cycles in a headwater stream: evidence of nocturnal bioturbation. Journal of Soils and Sediments 2016a; 16: 1815-1824, doi: 10.1007/s11368-016-1372-y.

Cooper RJ, Rawlins BG, Krueger T, Leze B, Hiscock KM, Pedentchouk N. Contrasting controls on the phosphorus concentration of suspended particulate matter under baseflow and storm event conditions in agricultural headwater streams. Sci Total Environ 2015b; 533: 49-59, doi: 10.1016/j.scitotenv.2015.06.113.

Crockford L, O'Riordain S, Taylor D, Melland AR, Shortle G, Jordan P. The application of high temporal resolution data in river catchment modelling and management strategies. Environ Monit Assess 2017; 189: 461, doi: 10.1007/s10661-017-6174-1.

Di HJ, Cameron KC. Nitrate leaching in temperate agroecosystems: sources, factors and mitigating strategies. Nutrient Cycling in Agroecosystems 2002; 46: 237-256.

Drake CW, Jones CS, Schilling KE, Amado AA, Weber LJ. Estimating nitrate-nitrogen retention in a large constructed wetland using high-frequency, continuous monitoring and hydrologic modeling. Ecological Engineering 2018; 117: 69-83, doi: 10.1016/j.ecoleng.2018.03.014.

Dupas R, Gascuel-Odoux C, Gilliet N, Grimaldi C, Gruau G. Distinct export dynamics for dissolved and particulate phosphorus reveal independent transport mechanisms in an arable headwater catchment. Hydrological Processes 2015a; 29: 3162-3178, doi: 10.1002/hyp.10432.

Dupas R, Minaudo C, Gruau G, Ruiz L, Gascuel-Odoux C. Multidecadal Trajectory of Riverine Nitrogen and Phosphorus Dynamics in Rural Catchments. Water Resources Research 2018; 54: 5327-5340, doi: 10.1029/2018wr022905.

Dupas R, Tavenard R, Fovet O, Gilliet N, Grimaldi C, Gascuel-Odoux C. Identifying seasonal patterns of phosphorus storm dynamics with dynamic time warping. Water Resources Research 2015b; 51: 8868-8882, doi: 10.1002/2015wr017338.

Edwards AC, Withers PJA. Transport and delivery of suspended solids, nitrogen and phosphorus from various sources to freshwaters in the UK. Journal of Hydrology 2008; 350: 144-153, doi: 10.1016/j.jhydrol.2007.10.053.

Fekete BM, Looser U, Pietroniro A, Robarts RD. Rationale for Monitoring Discharge on the Ground. Journal of Hydrometeorology 2012; 13: 1977-1986, doi: 10.1175/jhm-d-11-0126.1.

Halliday S, Skeffington R, Bowes M, Gozzard E, Newman J, Loewenthal M, et al. The Water Quality of the River Enborne, UK: Observations from High-Frequency Monitoring in a Rural, Lowland River System. Water 2014; 6: 150-180, doi: 10.3390/w6010150.

Halliday SJ, Skeffington RA, Wade AJ, Bowes MJ, Gozzard E, Newman JR, et al. High-frequency water quality monitoring in an urban catchment: hydrochemical dynamics, primary production and implications for the Water Framework Directive. Hydrological Processes 2015; 29: 3388-3407, doi: 10.1002/hyp.10453.

Halliday SJ, Wade AJ, Skeffington RA, Neal C, Reynolds B, Rowland P, et al. An analysis of long-term trends, seasonality and short-term dynamics in water quality data from Plynlimon, Wales. Sci Total Environ 2012; 434: 186-200, doi: 10.1016/j.scitotenv.2011.10.052.

Harvey GL, Henshaw AJ, Moorhouse TP, Clifford NJ, Holah H, Grey J, et al. Invasive crayfish as drivers of fine sediment dynamics in rivers: field and laboratory evidence. Earth Surface Processes and Landforms 2014; 39: 259-271, doi: 10.1002/esp.3486.

Inman A, Winter M, Wheeler R, Vrain E, Lovett A, Collins A, et al. An exploration of individual, social and material factors influencing water pollution mitigation behaviours within the farming community. Land Use Policy 2018; 70: 16-26, doi: 10.1016/j.landusepol.2017.09.042.

Jarvie HP, Neal C, Withers PJ. Sewage-effluent phosphorus: a greater risk to river eutrophication than agricultural phosphorus? Sci Total Environ 2006; 360: 246-53, doi: 10.1016/j.scitotenv.2005.08.038.

Jarvie HP, Sharpley AN, Kresse T, Hays PD, Williams RJ, King SM, et al. Coupling High-Frequency Stream Metabolism and Nutrient Monitoring to Explore Biogeochemical Controls on Downstream Nitrate Delivery. Environ Sci Technol 2018; 52: 13708-13717, doi: 10.1021/acs.est.8b03074.

Jones AS, Aanderud ZT, Horsburgh JS, Eiriksson DP, Dastrup D, Cox C, et al. Designing and Implementing a Network for Sensing Water Quality and Hydrology across Mountain to Urban Transitions. JAWRA Journal of the American Water Resources Association 2017; 53: 1095-1120, doi: 10.1111/1752-1688.12557.

Krause S, Lewandowski J, Dahm CN, Tockner K. Frontiers in real-time ecohydrology - a paradigm shift in understanding complex environmental systems. Ecohydrology 2015; 8: 529-537, doi: 10.1002/eco.1646.

Lewis MA. Borehole drilling and sampling in the Wensum Demonstration Test Catchment. British Geological Survey Commissioned Report CR/11/162 2014: 52

Lloyd CE, Freer JE, Johnes PJ, Collins AL. Using hysteresis analysis of high-resolution water quality monitoring data, including uncertainty, to infer controls on nutrient and sediment transfer in catchments. Sci Total Environ 2016a; 543: 388-404, doi: 10.1016/j.scitotenv.2015.11.028.

Lloyd CEM, Freer JE, Collins AL, Johnes PJ, Jones JI. Methods for detecting change in hydrochemical time series in response to targeted pollutant mitigation in river catchments. Journal of Hydrology 2014; 514: 297-312, doi: 10.1016/j.jhydrol.2014.04.036.

Lloyd CEM, Freer JE, Johnes PJ, Coxon G, Collins AL. Discharge and nutrient uncertainty: implications for nutrient flux estimation in small streams. Hydrological Processes 2016b; 30: 135-152, doi: 10.1002/hyp.10574.

Lovett AA, Hiscock KM, Outram FN, Cooper RJ, Dugdale S, Stevenson J, Sünnenberg G, Hama-Aziz Z, Dockerty TL, Noble L, Beamish J, Hovesen P. Experiments with cover crops and cultivation techniques in the Wensum DTC. Aspects of Applied Biology 2015; 129: 85-90.

Marin-Perez R, Garcia-Pintado J, Gomez AS. A real-time measurement system for long-life flood monitoring and warning applications. Sensors (Basel) 2012; 12: 4213-36, doi: 10.3390/s120404213.

McGonigle DF, Burke SP, Collins AL, Gartner R, Haft MR, Harris RC, et al. Developing Demonstration Test Catchments as a platform for transdisciplinary land management research in England and Wales. Environ Sci Process Impacts 2014; 16: 1618-1628, doi: 10.1039/c3em00658a.

Mellander P-E, Melland AR, Jordan P, Wall DP, Murphy PNC, Shortle G. Quantifying nutrient transfer pathways in agricultural catchments using high temporal resolution data. Environmental Science & Policy 2012; 24: 44-57, doi: 10.1016/j.envsci.2012.06.004.

Neal C, Reynolds B, Kirchner JW, Rowland P, Norris D, Sleep D, et al. High-frequency precipitation and stream water quality time series from Plynlimon, Wales: an openly accessible data resource spanning the periodic table. Hydrological Processes 2013; 27: 2531-2539, doi: 10.1002/hyp.9814.

Nimick DA, Gammons CH, Parker SR. Diel biogeochemical processes and their effect on the aqueous chemistry of streams: A review. Chemical Geology 2011; 283: 3-17, doi: 10.1016/j.chemgeo.2010.08.017.

Outram FN, Cooper RJ, Sunnenberg G, Hiscock KM, Lovett AA. Antecedent conditions, hydrological connectivity and anthropogenic inputs: Factors affecting nitrate and phosphorus transfers to agricultural headwater streams. Sci Total Environ 2016; 545-546: 184-99, doi: 10.1016/j.scitotenv.2015.12.025.

Outram FN, Lloyd CEM, Jonczyk J, Benskin CMH, Grant F, Perks MT, et al. High-frequency monitoring of nitrogen and phosphorus response in three rural catchments to the end of the 2011–2012 drought in England. Hydrology and Earth System Sciences 2014; 18: 3429-3448, doi: 10.5194/hess-18-3429-2014.

Palmer-Felgate EJ, Jarvie HP, Williams RJ, Mortimer RJG, Loewenthal M, Neal C. Phosphorus dynamics and productivity in a sewage-impacted lowland chalk stream. Journal of Hydrology 2008; 351: 87-97, doi: 10.1016/j.jhydrol.2007.11.036.

Rice SP, Johnson MF, Mathers K, Reeds J, Extence C. The importance of biotic entrainment for base flow fluvial sediment transport. Journal of Geophysical Research: Earth Surface 2016; 121: 890-906, doi: 10.1002/2015jf003726.

Rode M, Halbedel Nee Angelstein S, Anis MR, Borchardt D, Weitere M. Continuous In-Stream Assimilatory Nitrate Uptake from High-Frequency Sensor Measurements. Environ Sci Technol 2016a; 50: 5685-94, doi: 10.1021/acs.est.6b00943.

Rode M, Wade AJ, Cohen MJ, Hensley RT, Bowes MJ, Kirchner JW, et al. Sensors in the Stream: The High-Frequency Wave of the Present. Environ Sci Technol 2016b; 50: 10297-10307, doi: 10.1021/acs.est.6b02155.

Rozemeijer JC, Van der Velde Y, Van Geer FC, De Rooij GH, Torfs PJF, Broers HP. Improving load estimates for NO3 and P in surface waters by characterising the concentration response to rainfall events. Environmental Science & Technology 2010; 44: 8

Skeffington RA, Halliday SJ, Wade AJ, Bowes MJ, Loewenthal M. Using high-frequency water quality data to assess sampling strategies for the EU Water Framework Directive. Hydrology and Earth System Sciences 2015; 19: 2491-2504, doi: 10.5194/hess-19-2491-2015.

Strohmeier S, Knorr KH, Reichert M, Frei S, Fleckenstein JH, Peiffer S, et al. Concentrations and fluxes of dissolved organic carbon in runoff from a forested catchment: insights from high frequency measurements. Biogeosciences 2013; 10: 905-916, doi: 10.5194/bg-10-905-2013.

Stutter MI, Langan SJ, Cooper RJ. Spatial and temporal dynamics of stream water particulate and dissolved N, P and C forms along a catchment transect, NE Scotland. Journal of Hydrology 2008; 350: 187-202, doi: 10.1016/j.jhydrol.2007.10.048.

Turley MD, Bilotta GS, Gasparrini A, Sera F, Mathers KL, Humpheryes I, et al. The effects of non-native signal crayfish (Pacifastacus leniusculus) on fine sediment and sediment-biomonitoring. Sci Total Environ 2017; 601-602: 186-193, doi: 10.1016/j.scitotenv.2017.05.106.

UKTAG. Updated recommendations on environmental standards: River basin management (2015-21). UK Technical Advisory Group on the Water Framework Directive, 2013, pp. 80

Voulvoulis N, Arpon KD, Giakoumis T. The EU Water Framework Directive: From great expectations to problems with implementation. Sci Total Environ 2017; 575: 358-366, doi: 10.1016/j.scitotenv.2016.09.228.

Wade AJ, Palmer-Felgate EJ, Halliday SJ, Skeffington RA, Loewenthal M, Jarvie HP, et al. Hydrochemical processes in lowland rivers: insights from in situ, high-resolution monitoring. Hydrology and Earth System Sciences 2012; 16: 4323-4342, doi: 10.5194/hess-16-4323-2012.

Withers PJ, Jarvie HP. Delivery and cycling of phosphorus in rivers: a review. Sci Total Environ 2008; 400: 379-95, doi: 10.1016/j.scitotenv.2008.08.002.

Yang X, Jomaa S, Buttner O, Rode M. Autotrophic nitrate uptake in river networks: A modeling approach using continuous high-frequency data. Water Res 2019; 157: 258-268, doi: 10.1016/j.watres.2019.02.059.

Zimmer MA, Pellerin B, Burns DA, Petrochenkov G. Temporal Variability in Nitrate-Discharge Relationships in Large Rivers as Revealed by High-Frequency Data. Water Resources Research 2019; 55: 973-989, doi: 10.1029/2018wr023478.

TABLES

Table 1: EU Water Framework Directive (WFD) thresholds applied to the Blackwater Drain to assess its physico-chemical status (UKTAG, 2013).

Parameter	EU WFD Physico-chemical Status				
	Bad	**Poor**	**Moderate**	**Good**	**High**
Nitrate (mg N L^{-1})	>11.3	11.3 – 5.6	5.6 – 3.6	3.6 – 0.8	< 0.8
TRP (mg P L^{-1})	>1.003	1.003 – 0.173	0.173 – 0.069	0.069 – 0.036	<0.036
Dissolved oxygen (%)	<45	45 – 54	55 – 60	61 – 70	>70
Temperature (^{o}C)	>30	30 – 28	28 – 23	23 – 20	<20
pH	<4.89	4.89 – 5.44	5.44 – 5.95	5.95 – 6.60	>6.60

Table 2: Summary high-resolution (30 min) water quality data for the Blackwater Drain at site F for the period October 2011 – September 2018. Values presented as means with one standard deviation in parentheses.

Season/Flow	Discharge (m^3 s^{-1})	Temperature (^oC)	Conductivity (μS cm^{-1})	Dissolved Oxygen (%)	pH	Turbidity (NTU)	Chlorophyll (μg L^{-1})	Nitrate (mg N L^{-1})	Total Phosphorus (mg P L^{-1})	Total Reactive Phosphorus (mg P L^{-1})
Spring (MAM)	0.101 (0.097)	9.5 (2.8)	725 (28)	94 (9)	7.77 (0.10)	9.3 (6.7)	5.3 (1.9)	5.3 (1.4)	0.100 (0.041)	0.079 (0.024)
Summer (JJA)	0.039 (0.039)	14.0 (1.6)	718 (30)	86 (7)	7.72 (0.16)	7.5 (4.7)	5.2 (2.0)	4.3 (0.9)	0.109 (0.036)	0.093 (0.022)
Autumn (SON)	0.089 (0.093)	11.1 (2.3)	736 (29)	85 (9)	7.68 (0.13)	5.5 (4.7)	4.3 (1.2)	4.4 (1.4)	0.083 (0.035)	0.076 (0.023)
Winter (DJF)	0.162 (0.110)	6.1 (1.6)	752 (27)	96 (9)	7.82 (0.14)	7.4 (8.1)	5.1 (1.3)	6.4 (1.2)	0.082 (0.040)	0.068 (0.022)
Low flow (Q_{90})	0.019 (0.002)	13.8 (1.7)	724 (17)	85 (7)	7.71 (0.12)	7.3 (3.5)	4.4 (1.3)	4.1 (0.4)	0.109 (0.025)	0.095 (0.018)
High flow (Q_{10})	0.326 (0.136)	7.2 (2.2)	736 (52)	90 (8)	7.74 (0.15)	12.6 (15.3)	6.4 (2.3)	7.3 (1.8)	0.107 (0.079)	0.076 (0.039)
All	0.098 (0.099)	10.2 (3.5)	733 (31)	90 (10)	7.74 (0.15)	7.4 (6.3)	5.0 (1.7)	5.1 (1.5)	0.090 (0.039)	0.080 (0.024)

FIGURES CAPTIONS

Figure 1: Spatial variability in bedrock geology (BGS; 1:10,000), superficial geology (BGS; 1:10,000), land use (LCM2007) and soil type (LandIS) across the Blackwater Drain sub-catchment of the River Wensum, UK. Also showing the layout of field monitoring infrastructure and mini-catchment boundaries. Geological maps reproduced with the permission of the British Geological Survey, ©NERC; LCM2007© and database right NERC (CEH) 2011. All rights reserved. Contains Ordnance Survey data © Crown copyright and database right 2007. © third party licensors.

Figure 2: Photographs of a main Blackwater Drain monitoring station at site E (top left); site F looking downstream (top right); site F looking upstream (bottom right); and a minor river monitoring station at site C (bottom left).

Figure 3: High-resolution (30 min) time-series of hydrochemistry in the Blackwater Drain at site F for the period October 2011 – September 2018. Gaps in the data were caused by intermittent failure of the automated bankside monitoring equipment.

Figure 4: Diel cycles in the hydrochemistry of the Blackwater Drain at site F, differentiated by season. The central lines are the mean values of the entire high-resolution dataset recorded between October 2011 and September 2018, with the shading representing three standard errors.

Figure 5: Correlation panel plot of the Blackwater Drain hydrochemistry recorded under high flow (Q_{10}) conditions at site F between October 2011 and September 2018. The upper right section displays Pearson's correlation coefficients with the number size proportional to correlation strength. The bottom left panel shows the measurements (points) and linear regression (line). Central histograms show the distribution of each parameter.

Figure 6: Correlation panel plot of the Blackwater Drain hydrochemistry recorded under low flow (Q_{90}) conditions at site F between October 2011 and September 2018. The upper right section displays Pearson's correlation coefficients with the number size proportional to correlation strength. The bottom left panel shows the measurements (points) and linear regression (line). Central histograms show the distribution of each parameter.

Figure 7: Relationship between mean daily shallow (4 m depth) groundwater levels at Merrisons Lane and mean daily river discharge, nitrate concentration, total phosphorus concentration and turbidity in the Blackwater Drain at site F.

Figure 8: Seasonal relationships between daily precipitation total and the percentage change in daily discharge, nitrate concentration, total phosphorus concentration and turbidity in the Blackwater Drain at site F.

Figure 9: 3-D conceptual models of catchment hydrochemical processes during (left) winter and (right) summer in the Blackwater Drain. Blue arrows denote the major hydrological flow paths; black labels highlight the River Wensum DTC monitoring infrastructure; red boxes denote typical hydrochemical dynamics. A complementary conceptual model of hydrogeological processes in the Blackwater Drain is presented in Cooper et al. (2018).

Figure 10: EU Water Framework Directive status classifications for the Blackwater Drain at site F for the period October 2011 – September 2018 based on the 30-min resolution dataset.

Credit Author Statement

Richard Cooper – Conceptualization; methodology; formal analysis; investigation; data curation; writing – original draft; visualization.

Kevin Hiscock – Supervision; project administration; funding acquisition; writing – review & editing.

Andrew Lovett – Supervision; project administration; funding acquisition; writing – review & editing.

Stephen Dugdale – Investigation; resources

Gisela Sünnenberg – Investigation; resources

Emilie Vrain – Investigation; writing – original draft

Declaration of interests

☒ The authors declare that they have no known competing financial interests or personal relationships that could have appeared to influence the work reported in this paper.

☐The authors declare the following financial interests/personal relationships which may be considered as potential competing interests:

Highlights

- River Wensum Demonstration Test Catchment (DTC) established by UK government;
- Network of automated, *in-situ*, web-based sensor technologies deployed;
- 8.9 million hydrochemical measurements generated between 2011 and 2018;
- Hydrochemical dynamics at 30-minute to annual timescales explored;
- High-resolution data used to develop conceptual models of hydrochemical processes

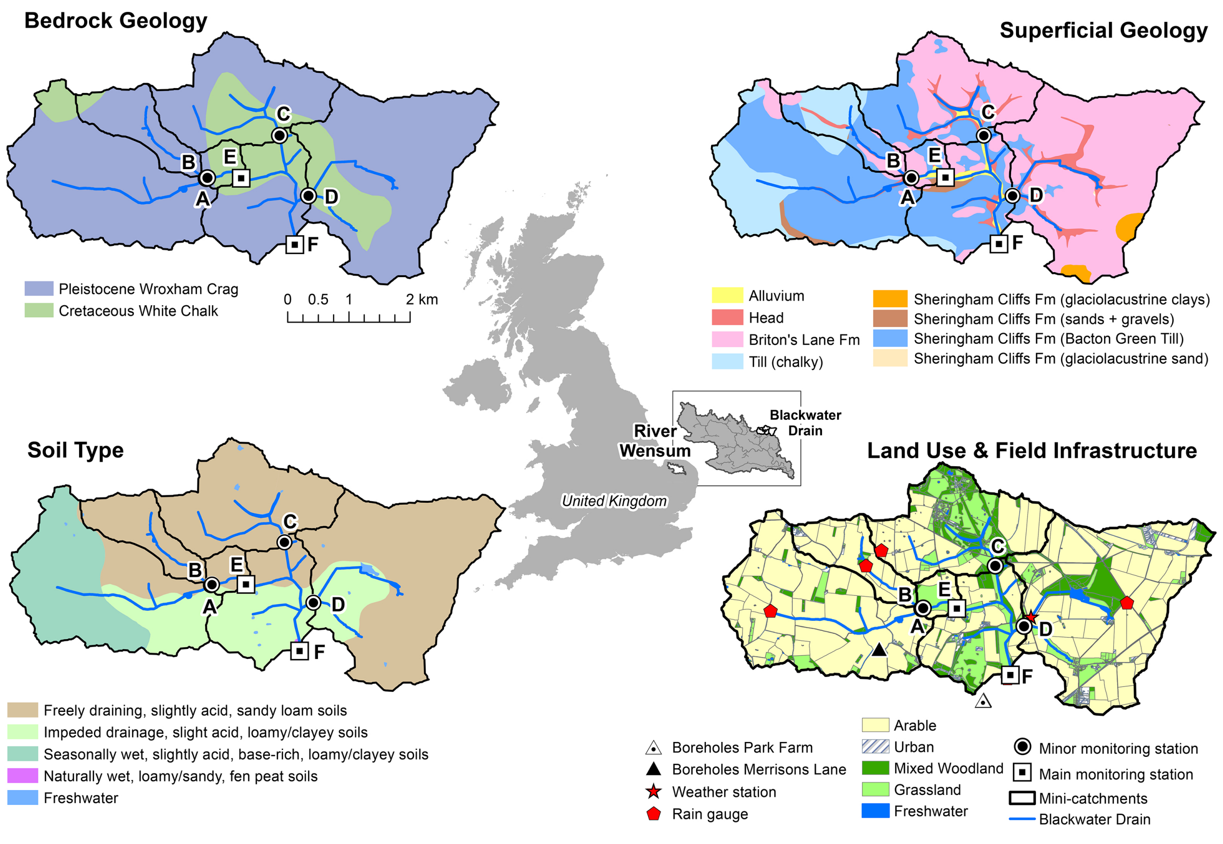

Bedrock Geology
Pleistocene Wroxham Crag
Cretaceous White Chalk
0 0.5 1 2 km
A
B
C
D
E
F
Superficial Geology
Alluvium
Head
Briton's Lane Fm
Till (chalky)
Sheringham Cliffs Fm (glaciolacustrine clays)
Sheringham Cliffs Fm (sands + gravels)
Sheringham Cliffs Fm (Bacton Green Till)
Sheringham Cliffs Fm (glaciolacustrine sand)
River Wensum
Blackwater Drain
United Kingdom
Soil Type
Freely draining, slightly acid, sandy loam soils
Impeded drainage, slight acid, loamy/clayey soils
Seasonally wet, slightly acid, base-rich, loamy/clayey soils
Naturally wet, loamy/sandy, fen peat soils
Freshwater
Land Use & Field Infrastructure
Boreholes Park Farm
Boreholes Merrisons Lane
Weather station
Rain gauge
Arable
Urban
Mixed Woodland
Grassland
Freshwater
Minor monitoring station
Main monitoring station
Mini-catchments
Blackwater Drain

Figure 1

Figure 2

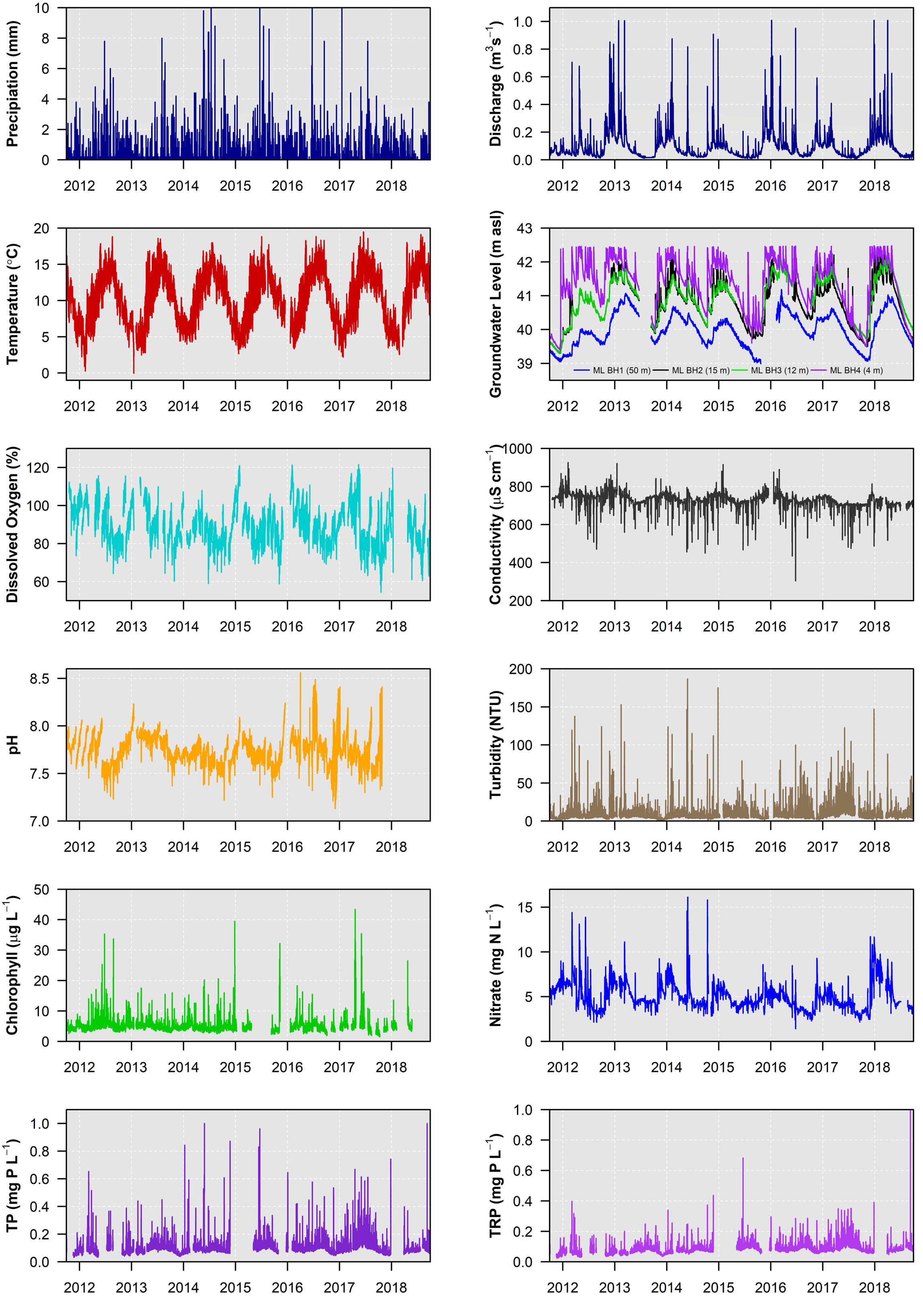

Precipiation (mm)
Discharge ($m^3 s^{-1}$)
Temperature (°C)
Groundwater Level (m asl)
ML BH1 (50 m)
ML BH2 (15 m)
ML BH3 (12 m)
ML BH4 (4 m)
Dissolved Oxygen (%)
Conductivity (μS cm^{-1})
pH
Turbidity (NTU)
Chlorophyll (μg L^{-1})
Nitrate (mg N L^{-1})
TP (mg P L^{-1})
TRP (mg P L^{-1})
2012 2013 2014 2015 2016 2017 2018

Figure 3

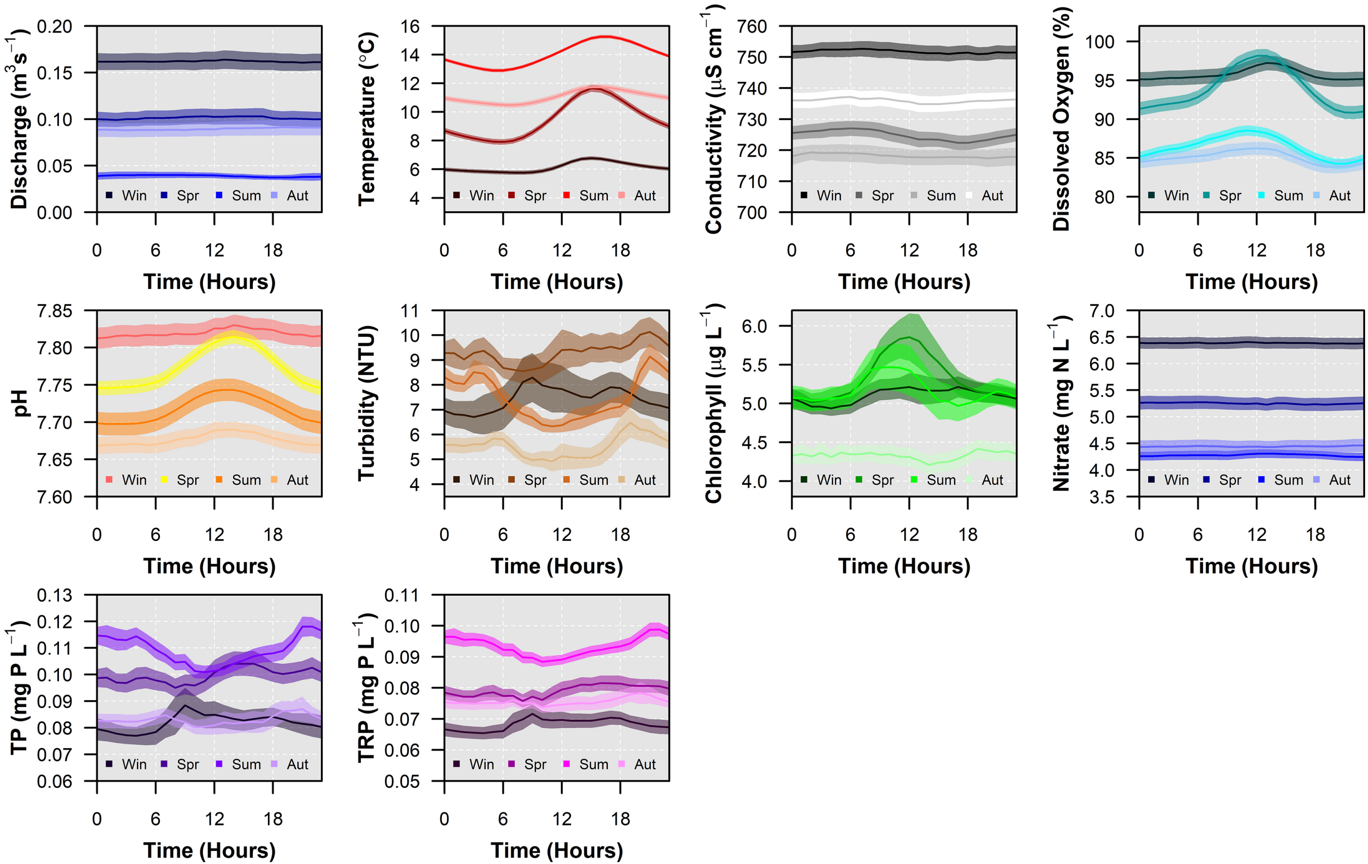
Discharge ($m^3 s^{-1}$)
Temperature (°C)
Conductivity (µS cm^{-1})
Dissolved Oxygen (%)
pH
Turbidity (NTU)
Chlorophyll (µg L^{-1})
Nitrate (mg N L^{-1})
TP (mg P L^{-1})
TRP (mg P L^{-1})
Time (Hours)
Win
Spr
Sum
Aut

Figure 4

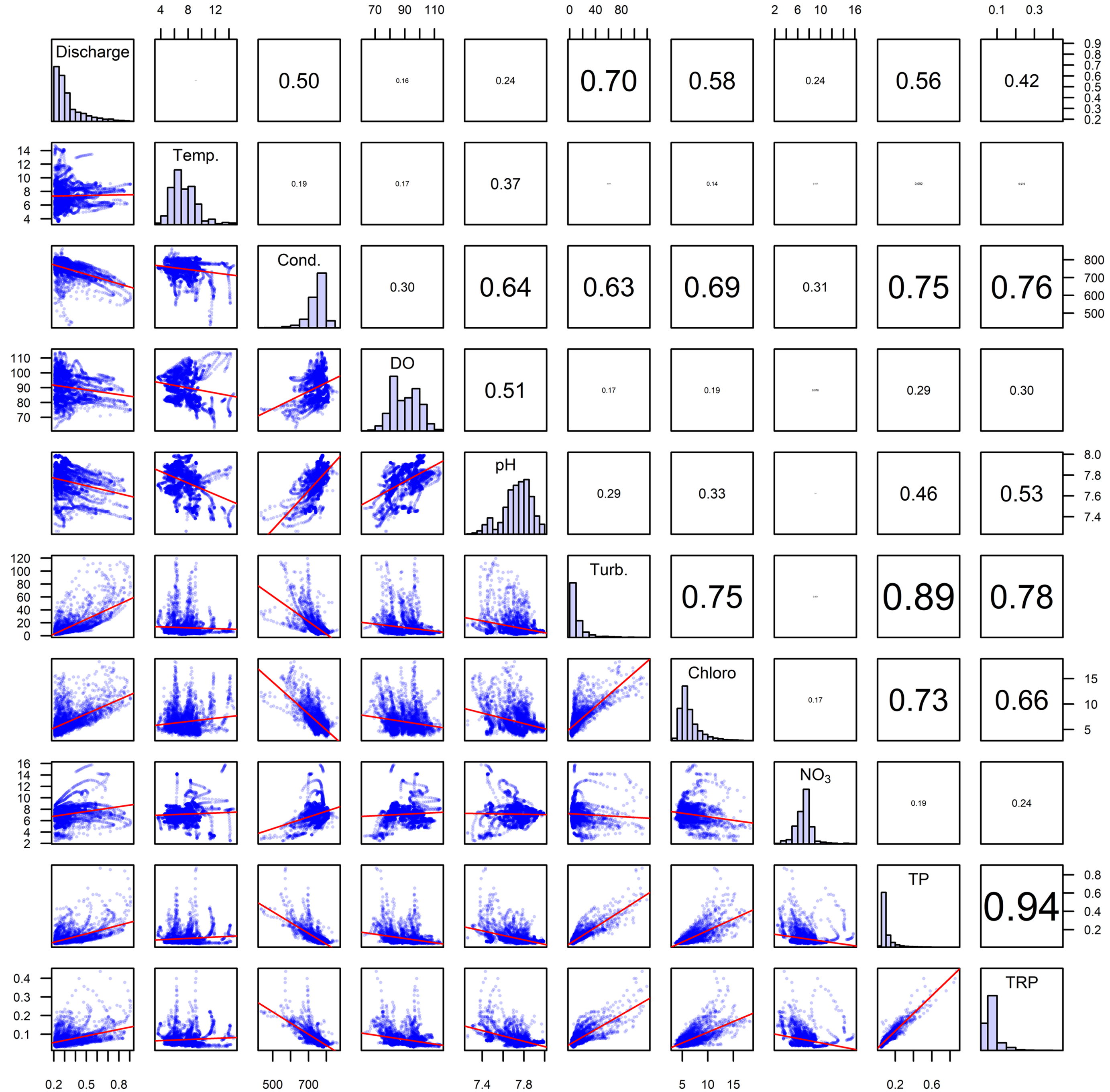
Discharge
Temp.
Cond.
DO
pH
Turb.
Chloro
NO_3
TP
TRP
0.50
0.16
0.24
0.70
0.58
0.24
0.56
0.42
0.19
0.17
0.37
0.14
0.30
0.64
0.63
0.69
0.31
0.75
0.76
0.51
0.17
0.19
0.29
0.30
0.29
0.33
0.46
0.53
0.75
0.89
0.78
0.17
0.73
0.66
0.19
0.24
0.94

Figure 5

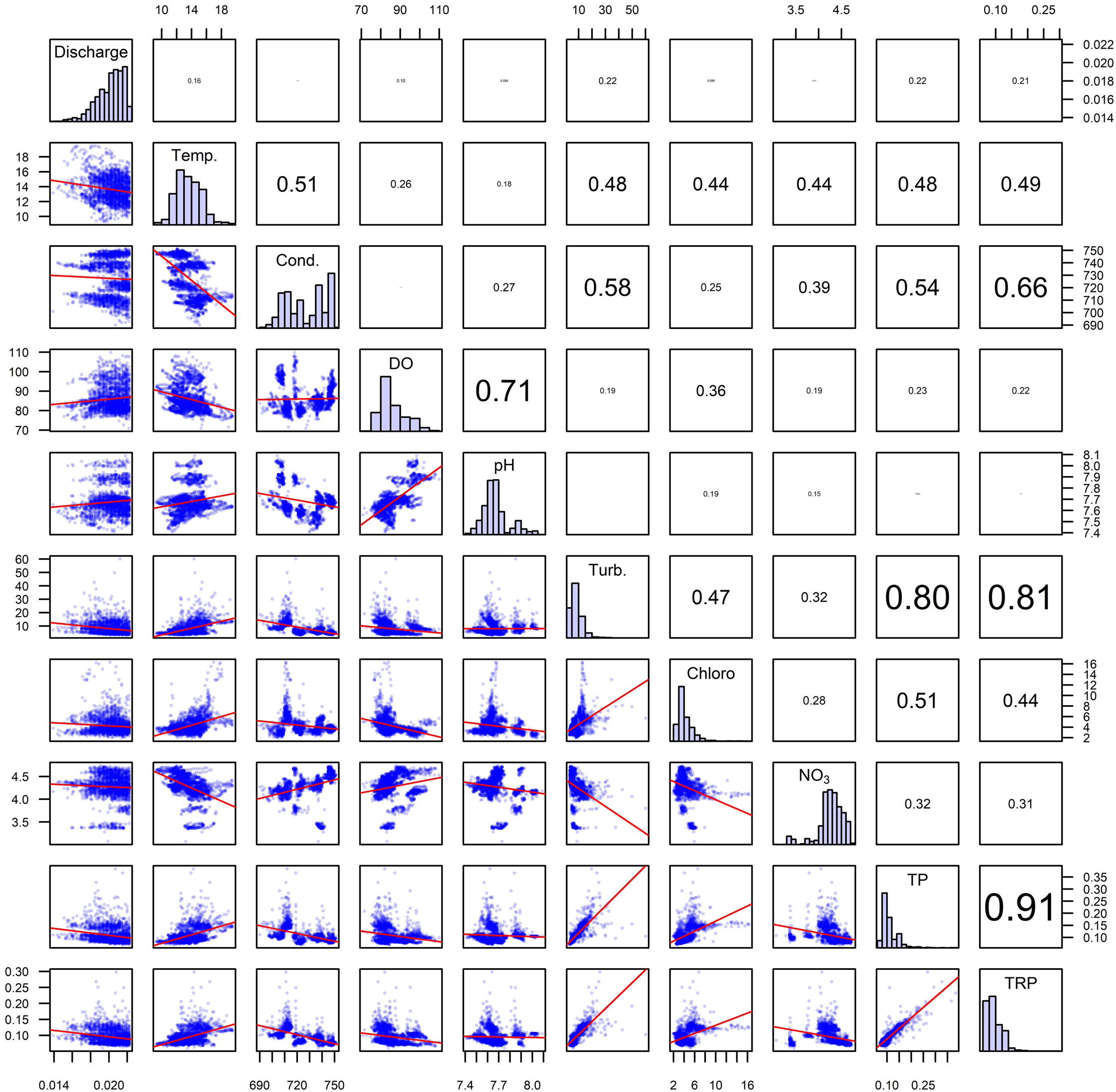

Discharge
Temp.
Cond.
DO
pH
Turb.
Chloro
NO_3
TP
TRP
0.16
0.22
0.22
0.21
0.51
0.26
0.18
0.48
0.44
0.44
0.48
0.49
0.27
0.58
0.25
0.39
0.54
0.66
0.71
0.19
0.36
0.19
0.23
0.22
0.19
0.15
0.47
0.32
0.80
0.81
0.28
0.51
0.44
0.32
0.31
0.91

Figure 6

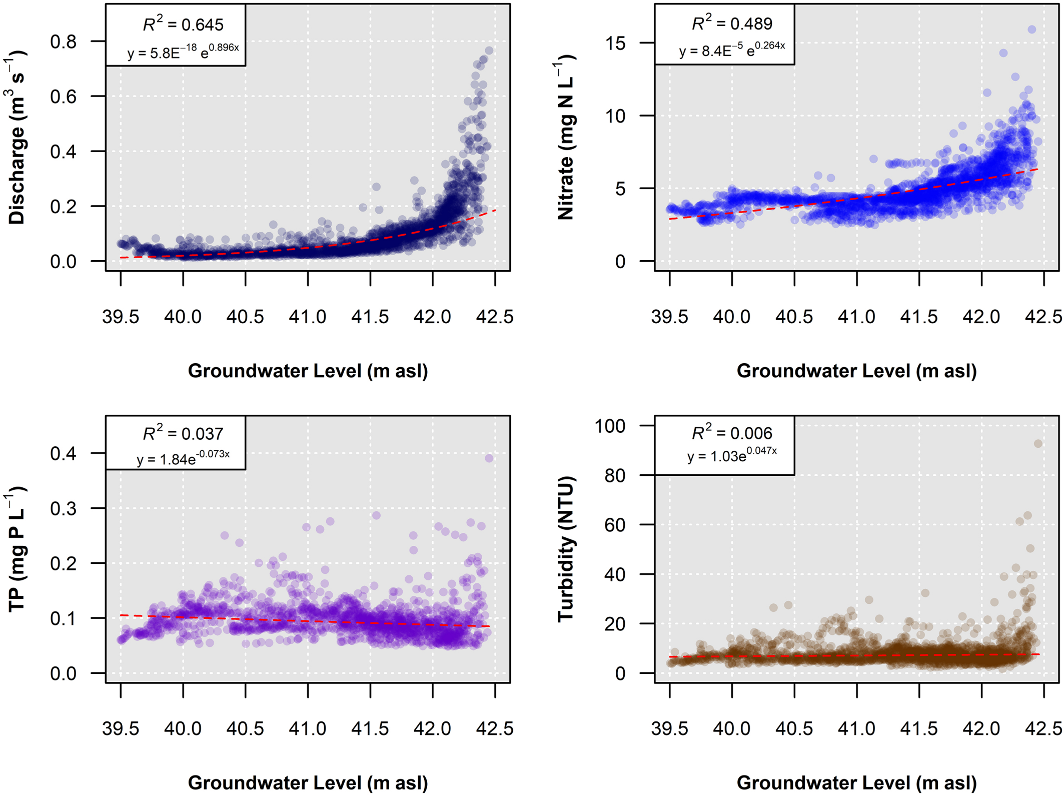

R² = 0.645
y = 5.8E−18 e^0.896x
Discharge (m³ s⁻¹)
Groundwater Level (m asl)
R² = 0.489
y = 8.4E−5 e^0.264x
Nitrate (mg N L⁻¹)
Groundwater Level (m asl)
R² = 0.037
y = 1.84e^-0.073x
TP (mg P L⁻¹)
Groundwater Level (m asl)
R² = 0.006
y = 1.03e^0.047x
Turbidity (NTU)
Groundwater Level (m asl)

Figure 7

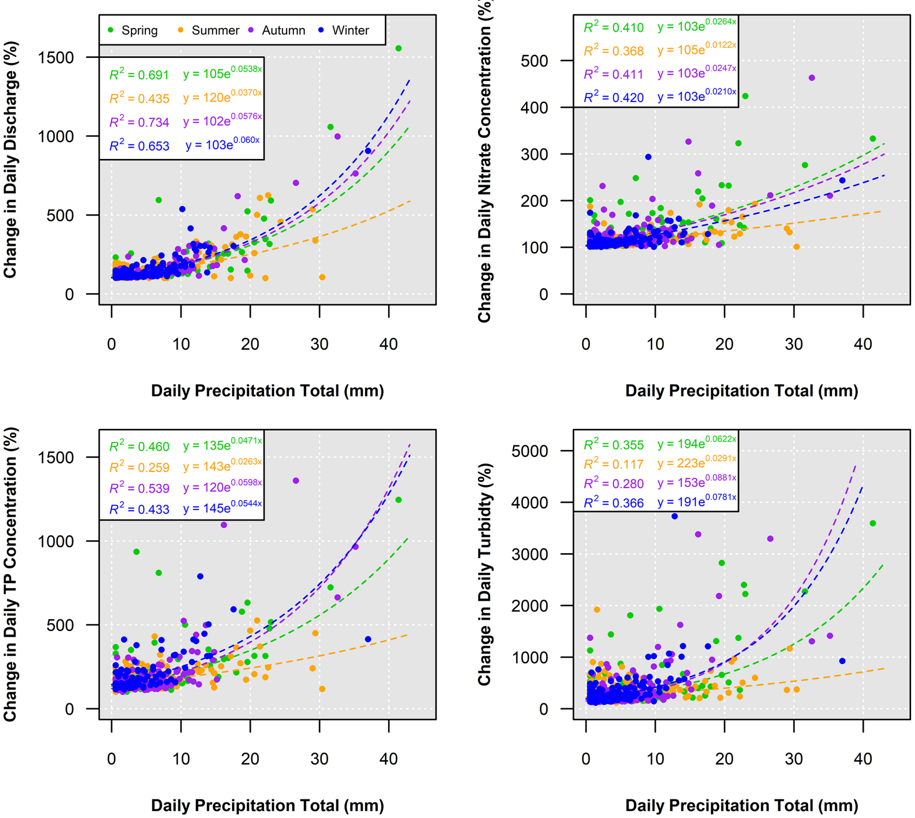

Spring
Summer
Autumn
Winter
R^2 = 0.691 y = 105e$^{0.0538x}$
R^2 = 0.435 y = 120e$^{0.0370x}$
R^2 = 0.734 y = 102e$^{0.0576x}$
R^2 = 0.653 y = 103e$^{0.060x}$
Change in Daily Discharge (%)
Daily Precipitation Total (mm)
R^2 = 0.410 y = 103e$^{0.0264x}$
R^2 = 0.368 y = 105e$^{0.0122x}$
R^2 = 0.411 y = 103e$^{0.0247x}$
R^2 = 0.420 y = 103e$^{0.0210x}$
Change in Daily Nitrate Concentration (%)
Daily Precipitation Total (mm)
R^2 = 0.460 y = 135e$^{0.0471x}$
R^2 = 0.259 y = 143e$^{0.0263x}$
R^2 = 0.539 y = 120e$^{0.0598x}$
R^2 = 0.433 y = 145e$^{0.0544x}$
Change in Daily TP Concentration (%)
Daily Precipitation Total (mm)
R^2 = 0.355 y = 194e$^{0.0622x}$
R^2 = 0.117 y = 223e$^{0.0291x}$
R^2 = 0.280 y = 153e$^{0.0881x}$
R^2 = 0.366 y = 191e$^{0.0781x}$
Change in Daily Turbidty (%)
Daily Precipitation Total (mm)

Figure 8

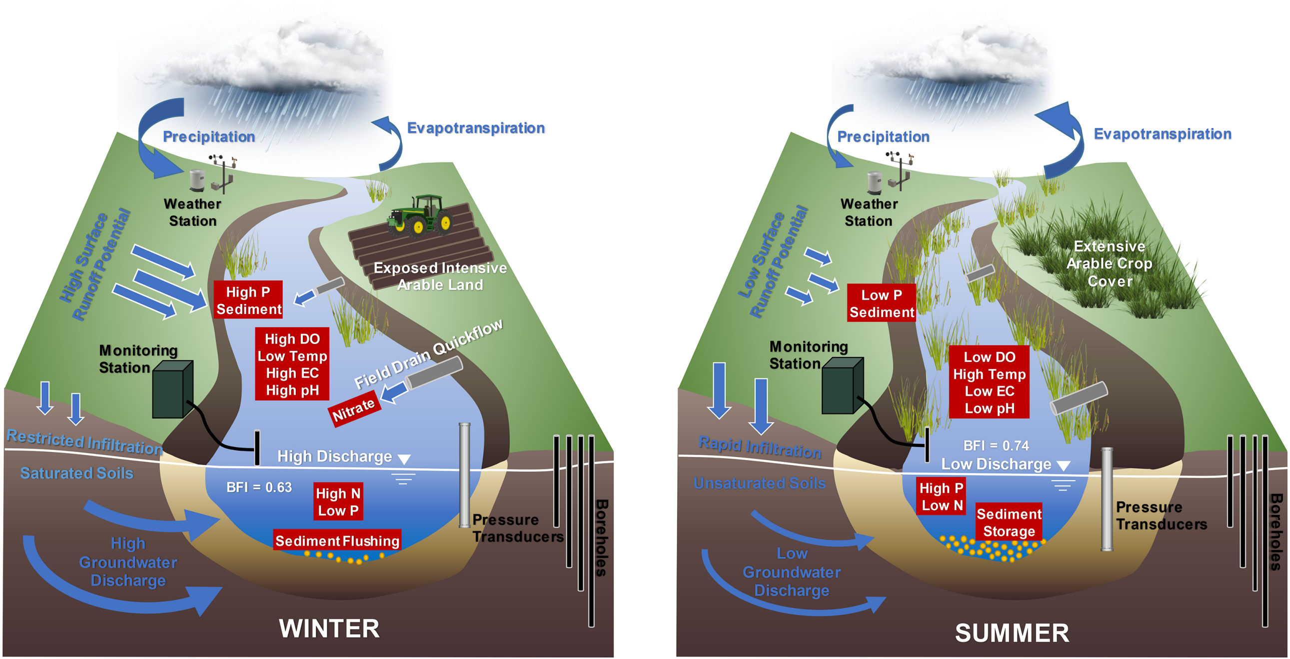

Precipitation
Evapotranspiration
Weather Station
High Surface Runoff Potential
Exposed Intensive Arable Land
High P Sediment
High DO
Low Temp
High EC
High pH
Field Drain Quickflow
Nitrate
Monitoring Station
Restricted Infiltration
Saturated Soils
High Discharge
BFI = 0.63
High N
Low P
Sediment Flushing
High Groundwater Discharge
Pressure Transducers
Boreholes
WINTER
Precipitation
Evapotranspiration
Weather Station
Low Surface Runoff Potential
Extensive Arable Crop Cover
Low P Sediment
Monitoring Station
Low DO
High Temp
Low EC
Low pH
Rapid Infiltration
BFI = 0.74
Low Discharge
Unsaturated Soils
High P
Low N
Sediment Storage
Low Groundwater Discharge
Pressure Transducers
Boreholes
SUMMER

Figure 9